available at www.sciencedirect.com

ScienceDirect

journal homepage: www.elsevier.com/locate/biochempharm

Involvement of sphingosine-1-phosphate and $S1P_1$ in angiogenesis: Analyses using a new $S1P_1$ antagonist of non-sphingosine-1-phosphate analog

Kiyoaki Yonesu [a,*], *Yumi Kawase* [a], *Tatsuya Inoue* [b], *Nana Takagi* [c], *Jun Tsuchida* [d], *Yoh Takuwa* [e], *Seiichiro Kumakura* [c], *Futoshi Nara* [a]

[a] *Exploratory Research Laboratories II, Daiichi Sankyo Co., Ltd., 1-16-13 Kitakasai, Edogawa-ku, Tokyo 134-8630, Japan*
[b] *Biological Research Laboratories II, Daiichi Sankyo Co., Ltd., Japan*
[c] *Biological Research Laboratories III, Daiichi Sankyo Co., Ltd., Japan*
[d] *Intellectual Property Department, Daiichi Sankyo Co., Ltd., Japan*
[e] *Department of Physiology, Kanazawa University Graduate School of Medicine, 13-1 Takara-machi, Kanazawa, Ishikawa 920-8640, Japan*

ARTICLE INFO

Article history:
Received 29 October 2008
Accepted 15 December 2008

Keywords:
Angiogenesis inhibitor
Sphingosine-1-phosphate (Sph-1-P)
Endothelial differentiation gene-1 (Edg-1/$S1P_1$)
Tube formation
Anti-arthritis

ABSTRACT

Chemical lead 2 (CL2) is the first non-sphingosine-1-phosphate (Sph-1-P) analog type antagonist of endothelial differentiation gene-1 (Edg-1/$S1P_1$), which is a member of the Sph-1-P receptor family. CL2 inhibits [^{3}H]Sph-1-P/$S1P_1$ binding and shows concentration-dependent inhibition activity against both intracellular cAMP concentration decrease and cell invasion induced by the Sph-1-P/$S1P_1$ pathway. It also inhibits normal tube formation in an angiogenesis culture model, indicating that CL2 has anti-angiogenesis activity. This compound improved the disease conditions in two angiogenic models *in vivo*. It significantly inhibited angiogenesis induced by vascular endothelial growth factor in a rabbit cornea model as well as the swelling of mouse feet in an anti-type II collagen antibody-induced arthritis model. These results indicate that the Sph-1-P/$S1P_1$ pathway would have an important role in disease-related angiogenesis, especially in the processes of migration/invasion and tube formation. In addition, CL2 would be a powerful tool for the pharmacological study of the mechanisms of the Sph-1-P/$S1P_1$ pathway in rheumatoid arthritis, diabetes retinopathy, and solid tumor growth processes.

1. Introduction

If mammalian tissues suffer a lack of nutrients and/or oxygen, new blood vessels develop from parts of the surrounding tissues. This physiological phenomenon is called angiogenesis [1,2]. In normal adults, angiogenesis is a rare event except in the cases of wound healing and menstruation. Such angiogenesis is well-regulated and is useful for the maintenance of an individual's homeostasis. On the other hand, it is thought that angiogenesis is closely related to the progression of a

* *Corresponding author*. Tel.: +81 3 3680 0151; fax: +81 3 5696 8926.
E-mail address: yonesu.kiyoaki.t8@daiichisankyo.co.jp (K. Yonesu).

Abbreviations: bFGF, basic fibroblast growth factor; CHO, Chinese hamster ovary; CL2, chemical lead 2; dhfr, dihydrofolate reductase; Edg-1/$S1P_1$, endothelial differentiation gene-1; FBS, fetal bovine serum; FLIPR, fluorometric imaging plate reader; HEK293, human embryonic kidney 293; homo KO, homozygous knockout; HUVEC, human umbilical vein endothelial cells; IBMX, 3-isobutyl-1-methylxanthine; LPS, lipopolysaccharide; MTX, methotrexate; NZW, New Zealand white; Sph-1-P, sphingosine-1-phosphate; VEGF, vascular endothelial growth factor.

0006-2952/$ – see front matter
doi:10.1016/j.bcp.2008.12.007

number of diseases, including solid tumor growth [3,4], diabetes retinopathy [5], and chronic rheumatoid arthritis [6].

A malignant tumor can grow to a few millimeters in diameter with no blood supply [3]. Afterwards, it secretes vascular endothelial growth factor (VEGF), basic fibroblast growth factor (bFGF), other growth factors, and cytokines so that the surrounding tissues make new blood vessels [7,8]. The tumor then uses the newly formed vessels to grow itself, finally metastasizing to distant tissues or organs. Recently, an anti-human VEGF antibody called Avastin (Genentech, Inc., South San Francisco, USA) was launched as a drug for metastatic colorectal carcinoma. The VEGF receptor inhibitor Sutent (Pfizer Inc., NY, USA) is now also available for metastatic gastrointestinal stromal tumors and metastatic renal cell carcinoma.

Diabetes retinopathy is a major complication of diabetes and is the top cause of adult blindness [9,10]. Chronic hyperglycemia damages the retinal blood capillaries and the injured capillaries repeat the bleeding-and-angiogenesis cycle, along with fiber formation. Then the fibers shrink, finally causing retinal detachment [11,12].

In the case of rheumatoid arthritis, inflammatory cells (macrophages and T lymphocytes) infiltrate into articular cavities releasing inflammatory and angiogenic factors, such as bFGF, VEGF, tumor necrosis factor-α, and interleukin-1. In response to these factors, synovial cells grow and form a pannus. The pannus increases in size by angiogenesis and vigorously discharges matrix metalloproteinases, finally digesting the articular cartilage [13,14].

Sphingosine-1-phosphate (Sph-1-P), a plasma lipid, has a promoting effect on vascular endothelial cell growth, migration, and tube formation [15,16]. Sph-1-P is considered to be an important growth factor for endothelial cells because it acts in all three of the steps necessary for angiogenesis: growth, migration, and tube formation. Recently, it has been revealed that Sph-1-P exhibits this action through the endothelial differentiation gene-1 (Edg-1/$S1P_1$) [17] and to some extent with other S1P members, from $S1P_2$ to $S1P_5$ [18]. $S1P_1$ was discovered in phorbol 12-myristate 13-acetate-stimulated human umbilical vein endothelial cells (HUVEC) and is thought to be involved in the differentiation of endothelial cells [19]. After the identification of its natural ligand, experimental data showing that $S1P_1$ is involved in angiogenesis was reported, as follows. Similar to endothelial cells, Chinese hamster ovary (CHO) cells expressing $S1P_1$ migrated as a result of low concentrations of Sph-1-P (1–10 nM) [20,21]. Human embryonic kidney 293 (HEK293)-*edg-1* cells also migrated as a result of 10–100 nM Sph-1-P [15]. These findings show that $S1P_1$ has chemotactic activity *in vitro*. $S1P_1$ is mostly coupled with G_i protein and is thought to send cell growth, survival, and differentiation signals. Some research has demonstrated *in vitro* signal cross-talking between $S1P_1$ and growth factor receptors related to angiogenesis, such as platelet-derived growth factor receptor [22] and VEGF receptor [23]. Sph-1-P actually induced angiogenesis in an *in vivo* model, in which anti-$S1P_1$ antibody negated the effect [24]. It has also been reported that $S1P_1$ homozygous knockout (homo KO) is lethal in embryonic mice because of incomplete blood vessel development [25]. The knockout mice also showed abnormal limb development [26]. These studies indicate the Sph-1-P/$S1P_1$ pathway has an important role in angiogenesis.

In this report, we evaluated the synthetic $S1P_1$ antagonist chemical lead 2 (CL2) by a number of *in vitro* and *in vivo* assays in order to clarify the role of the Sph-1-P/$S1P_1$ pathway in disease-related angiogenesis.

2. Materials and methods

2.1. Reagents and animals

CL2, sodium 2-(4-ethoxyphenoxy)-5-(3-octadecyl-5-oxo-4,5-dihydro-1*H*-pyrazol-1-yl)benzenesulfonate, was synthesized in Exploratory Chemistry Research Laboratories, Sankyo Co., Ltd. (former company name before the merger, Shinagawa, Japan). NaCl and $MgCl_2$ were purchased from Nacalai Tesque (Chukyo, Japan). [^{35}S]GTPγS was purchased from PerkinElmer Japan Co., Ltd. (Yokohama, Japan). The cell culture plates were purchased from Corning International K.K. (Minato, Japan). Saline was purchased from Otsuka Pharmaceutical Co., Ltd. (Chiyoda, Japan). All other reagents were supplied by Sigma–Aldrich Japan (Shinagawa, Japan) unless otherwise stated. Six-week-old male Balb/c mice were purchased from Charles River Laboratories Japan, Inc. (Kohoku, Japan). Male New Zealand white (NZW) albino rabbits, with mean average body weights of 2.5 kg, were provided from Japan SLC, Inc. (Hamamatsu, Japan). The animals were maintained in a room controlled at a temperature and relative humidity of 24 ± 2 °C and 40–70%, respectively, and given food and water *ad libitum*. The experimental protocols were approved by the Ethics Review Committee for Animal Experimentation of Sankyo Co., Ltd. (Shinagawa, Japan).

2.2. Cloning of human $S1P_1$ cDNA and plasmid construction

The plasmid pME18S was kindly supplied by Dr. Handa of the Tokyo Institute of Technology (Meguro, Japan). The entire coding region of human $S1P_1$ was amplified from human aorta marathon-ready cDNA (Clontech Laboratories, Inc., Mountain View, USA) using the primers 5′-CCGCTCGAGCGGATGGGGCC-CACCAGCGTCCCGCTGGTCAAGGCC-3′ and 5′-ATAAGAATGC-GGCCGCTAAACTATCTAGGAAGAAGAGTTGACGTTTCCAGAA-GACAT-3′. The PCR product was subcloned into the *Xho* I–*Not* I site of pME18S and verified by sequencing. The obtained sequence was the same as that in the RefSeq (GenBank accession no. NM001400). This construct was named p*edg*-1-2.

2.3. Establishment of a cell line stably expressing human $S1P_1$

The CHO-*dhfr*$^{-/-}$ cells were also supplied by Dr. Handa. The plasmid pEIVWT-DHFR [27], which carries the dihydrofolate reductase (dhfr) gene was provided by Dr. Nishigaki (Daiichi Sankyo Co., Ltd., Shinagawa, Japan). Sph-1-P was purchased from BIOMOL International, L.P. (Plymouth Meeting, USA). A plasmid mixture of p*edg*-1-2 and pEIVWT-DHFR (10:1, w/w) was transfected into the CHO-*dhfr*$^{-/-}$ cells with LipofectAmine Plus Reagent (Invitrogen Japan K.K., Minato, Japan). The next

day, the cells were resuspended into selection medium [α-Minimum Essential Medium without ribonucleosides and deoxyribonucleosides (Invitrogen Japan K.K., Minato, Japan) containing 10% dialyzed fetal bovine serum (FBS) (SAFC Biosciences, Lenexa, USA), 100 units/mL penicillin G sodium (Invitrogen Japan K.K., Minato, Japan), and 100 μg/mL streptomycin sulfate (Invitrogen Japan K.K., Minato, Japan)] at a low cell density, and then plated in culture dishes. After 2 weeks, during which the medium was changed several times, about 50 single clones were picked up and cultured separately. The Sph-1-P reactivity of each clone was measured by [^{35}S]GTPγS binding assay [28] and the highest active clones were selected for each of the studies and named CHO-S1P$_1$ cells.

For gene amplification [29], the CHO-S1P$_1$ cells were cultured in a selection medium with 5 nM methotrexate (MTX) as a first selection step, then 25 nM, finally with 125 nM MTX. Subsequently, the CHO-S1P$_1$ cells that were resistant to the 125 nM MTX were maintained in the same selection medium until the following studies were performed.

For the establishment of a negative control cell line, pME18S and pEIVWT-DHFR (10:1, w/w) were transfected into the CHO-*dhfr*$^{-/-}$ cells, and 5 clones were selected and amplified by the same method. One of these clones was designated as CHO-mock cells and was maintained in the selection medium with 125 nM MTX.

2.4. *In vitro* membrane-binding assay

The synthesis of [3-^{3}H]Sphingosine was performed by GE Healthcare Bio-Sciences KK (Shinjuku, Japan). HEK293 cells which overexpress mouse sphingosine kinase 1a (mSPHK1a-HEK) [30] were generously provided by Dr. Kohama (Daiichi Sankyo. Co., Ltd., Shinagawa, Japan). [^{3}H]Sph-1-P was synthesized enzymatically according to the method of Kohama et al. [30] with modification. A total of 3.7 MBq of [3-^{3}H]sphingosine was converted to [^{3}H]Sph-1-P by the cytosol of mSPHK1aHEK cells in a reaction buffer [100 mM potassium-phosphate buffer, pH 7.4, 1 mM EDTA, pH 7.4, 15 mM NaF, 10 mM ATP, 5 mM $MgCl_2$, 1 mM 2-mercaptoethanol, 1 mM Na_3VO_4, 0.5 mM 4-deoxypyridoxine, 10% (v/v) glycerol]. The extraction of [^{3}H]Sph-1-P was performed by the modified method of Yatomi et al. [31]. After incubating for 4 h at 37 °C, the pH was lowered to less than 3 with HCl and any contaminants were removed by extraction with 3 times the volume of chloroform/methanol (2:1). The upper aqueous phase was collected and the pH was raised to more than 9 with NH_4OH. Then the product [^{3}H]Sph-1-P was extracted 4 times with an equal volume of chloroform. Each lower organic phase was recovered and dried and the remainder, i.e., [^{3}H]Sph-1-P, was resuspended in 80% (v/v) ethanol and stored at −20 °C until use. A part of [^{3}H]Sph-1-P was separated with TLC using 1-butanol/acetic acid/water (3:1:1, v/v/v) mobile phase and the Rf value of [^{3}H]Sph-1-P was confirmed to be 0.5, the same as unlabeled Sph-1-P standard.

The membrane preparation from CHO cells was performed by the modified method of Davaille et al. [32]. The CHO-S1P$_1$ or CHO-mock cells were sonicated in buffer A (5 mM Tris–HCl, pH 7.4, 1 mM EDTA, pH 7.4, 1 mM EGTA, pH 7.4, 0.25 M sucrose, 0.18 mg/mL phenylmethanesulfonyl fluoride, 50 μg/mL leupeptin), centrifuged at 2000 × *g* for 10 min at 4 °C. The supernatant was ultracentrifuged at 160,000 × *g* for 1 h at 4 °C. The precipitated membranes were resuspended in buffer B (20 mM HEPES, pH 7.4, 1 mM EDTA, pH 7.4, 100 mM NaCl, 10 mM $MgCl_2$), divided into small amounts, frozen in liquid nitrogen, and stored at −80 °C until use.

The *in vitro* membrane-binding assay was performed according to the method of Im et al. [33] with modification. The [^{3}H]Sph-1-P (40,000 dpm), membrane fraction (5 μg) from CHO-S1P$_1$ or CHO-mock cells and 80% (v/v) ethanol with or without 10 μM Sph-1-P were incubated for 30 min at 25 °C in the ×1 buffer [25 mM Tris–HCl, pH 7.4, 5 mM EDTA, pH 7.4, 100 mM NaCl, 15 mM NaF, 0.25 mM 4-deoxypyridoxine, 50 μg/mL fatty acid-free BSA, 0.005% (v/v) Tween 20, 1 tablet of protease inhibitor cocktail Complete, EDTA-free (Roche Diagnostics K.K., Minato, Japan), per 50 mL of buffer]. The reaction mixtures were filtrated with GF/B filters (PerkinElmer Japan Co., Ltd., Yokohama, Japan) and washed 3 times with wash buffer (25 mM Tris–HCl, pH 7.4, 100 μg/mL fatty acid-free BSA). At this time, the radioactivity bound on the filters was measured ($n = 4$). For the measurement of the inhibition activity of CL2, the [^{3}H]Sph-1-P (40,000 dpm), membrane fraction (5 μg) from CHO-S1P$_1$ cells, various amounts of CL2 and 80% (v/v) ethanol with or without 10 μM Sph-1-P were mixed, and the binding assay was performed as described above. Inhibition (%) of [^{3}H]Sph-1-P binding was calculated by the numerical expression $[1 - (A - B)/(C - B)] \times 100$, where *A*, *B*, and *C* represent the mean values (dpm) in the CL2-treated group, 10 μM Sph-1-P-addition group, and 80% (v/v) ethanol-addition group, respectively. The *A* value shows the total binding activity with the indicated amounts of CL2. The *B* value shows the non-specific binding activity. The *C* value shows the total binding activity without CL2.

2.5. cAMP assay

The measurement of the intracellular cAMP concentration was performed based on the method of Gong et al. [34] with modification. The CHO-S1P$_1$ cells were seeded into a 96-well plate (4×10^5 cells/well) with the selection medium and cultured overnight. The next day, the medium was changed to a serum-free one and the cells were preincubated with 1 mM 3-isobutyl-1-methylxanthine (IBMX) for 5 min at 37 °C, and then stimulated with or without 30 μM forskolin, 100 nM Sph-1-P and the indicated amounts of CL2 in the presence of 1 mM IBMX for 15 min at 37 °C. After the reaction, the cells were dissolved using 100 μL of 1% (v/v) Triton X-100 and the cAMP concentration was measured in a competitive assay using a cAMP femtomolar kit (CIS Bio International, Gif-sur-Yvette, France), following the instructions of the manufacturer ($n = 3$).

2.6. Screening of S1P$_1$ antagonists

High-throughput screening of our in-house compound library using a [^{3}H]Sph-1-P/S1P$_1$ binding assay was performed utilizing almost the same procedure as in the *in vitro* membrane-binding assay, except for the incubation for 1 h at 4 °C in × 1 buffer containing 300 mM mannitol to stabilize the membrane fraction from CHO-S1P$_1$ cells. The compounds which showed more than 70% inhibition of [^{3}H]Sph-1-P/S1P$_1$ binding at 25 μg/mL were evaluated by a manual *in vitro*

membrane-binding assay. The compounds which showed more than 70% inhibition at 10 μg/mL were picked up and re-evaluated in the cAMP assay. The compounds which showed more than 70% inhibition of intracellular cAMP concentration decreases stimulated by Sph-1-P at 10 μg/mL were considered to be $S1P_1$ antagonists and were further investigated.

2.7. Cell invasion assay

A cell invasion assay was performed according to the method of Rikitake et al. [35] with modification. BD BioCoat®, BD Matrigel® Growth Factor Reduced Matrigel Invasion Chambers were purchased from BD Biosciences (San Jose, USA). The invasion assay was performed in the selection medium without FBS. The 5×10^4 of CHO-$S1P_1$ cells mixed with the indicated amounts of CL2 were added to the upper chamber and 10 nM Sph-1-P was added to the lower one. After 16 h of incubation at 37 °C, the invaded cells (i.e., cells that had passed through the 8 μm pore size Matrigel-coated filter) were fixed with formalin/PBS and stained with Diff-Quik (Sysmex, Kobe, Japan). For each filter, the sum of the stained cells within 4 random microscopic fields (×100 power) was counted visually and represented as the extent of the cell invasion (cells/4 power fields, $n = 3$).

2.8. Cell growth inhibition assay

The CHO-$S1P_1$ cells were seeded into a 96-well plate (4×10^5 cells/well) with selection medium and cultured overnight. The next day, the medium was changed to a serum-free one and various amounts of CL2 were added to make final concentrations of up to 16.3 μM. The cells were then incubated for 22 h at 37 °C. A 20 μL aliquot of Alamar Blue (Serotec Ltd., Kidlington, UK) was added to each well and the cells were further incubated for 23 h at 37 °C. Finally, the fluorescence intensity of each well was measured (excitation 530 nm/emission 590 nm, $n = 4$). The obtained intensity indicates the cell growth. No self-fluorescence of CL2 was observed.

2.9. Angiogenesis culture model

An Angiogenesis Kit was purchased from KURABO industries Ltd. (Chuo, Japan). The pre-seeded human fibroblasts and HUVEC in the kit were co-cultured for 11 days using the medium which came with the kit. According to the manufacturer's protocol, on Days 1, 4, 7, and 9, the medium was changed to a new one containing 0, 3.3, or 16.3 μM CL2. On the final day, both cell types were fixed with ethanol and the HUVEC were additionally stained with anti-human von Willebrand factor antibodies which came with the kit. Images of the tubular HUVEC were micrographed (×200 power).

2.10. Measurement of Sph-1-P receptor specificity

The antagonistic activity of CL2 against G-protein coupled receptors other than Sph-1-P receptors was investigated in a PharmaScreen assay by MDS Pharma Services (http://www.mdsps.com/). The antagonistic activity of CL2 to $S1P_1$, $S1P_2$, and $S1P_3$ was measured with a fluorometric imaging plate reader (FLIPR) according to our previous report [36].

2.11. In vivo anti-angiogenesis assay in rabbit cornea model

One microgram of VEGF and the indicated amount of either CL2, SU-5416 (a VEGF receptor-signaling inhibitor) or vehicle (DMSO) were mixed with polyhydroxyethylmethacrylate to form sustained release pellets (Hydron pellets). The pellets were implanted into the corneas of albino rabbits (NZW, male, mean average body weight 2.5 kg, $n = 2$–5). After 7 days, the newborn blood vessels in the corneas were photographed and the total lengths were measured ($n = 8$–20).

2.12. Mouse anti-type II collagen antibody arthritis model

An Arthritogenic mAb Cocktail Kit was purchased from Chondrex, Inc. (Redmond, USA). The induction of arthritis was performed according to the instructions of the manufacturer. Balb/c mice (male, 7 weeks after birth) were divided into 5 groups ($n = 10$). On Day 0, the mice from groups 2 to 5 were sensitized by *i.v.* injection of an anti-type II collagen antibody cocktail. On Day 3, arthritis was induced by *i.p.* administration of lipopolysaccharide (LPS). On Days 3 through 13, the compounds [group 1, none; group 2, 0.5% (w/v) tragacanth (*p.o.*); group 3, saline (*i.p.*); group 4, 10 mg/kg CL2 dissolved in 0.5% (w/v) tragacanth (*p.o.*); and group 5, 10 mg/kg CL2 dissolved in saline (*i.p.*)] were administered daily. On Days 0, 3, 5, 7, 10, and 14, the body weight was measured and the swelling of the hind limbs was evaluated. The swelling score is the sum of the evaluations of both hind limbs (max. of total score = 6). Scoring criteria: one toe swelling = 1; more than one toe swelling = 2; remarkable swelling of instep = 3. For group 1, neither antibody nor LPS was administered. For an anti-inflammatory reference drug, 5 mg/kg indomethacin dissolved in 0.5% (w/v) tragacanth was *p.o.* administered on Days 0 through 13 ($n = 10$).

2.13. Measurement of CL2 concentration in mice plasma in vivo

A total of 10 mg/kg CL2 dissolved in distilled water was administered to Balb/c mice (male, 6-week-old, $n = 3$) by *p.o.* or *i.p.* The plasma concentrations of CL2 were measured by Daiichi Sankyo RD Associe Co., Ltd. (http://www.daiichisan-kyo-rda.jp/index.html), and the value of the area under the curve (μg h/mL) was calculated.

2.14. Statistical analysis

The statistical significance of the differences between the mean values was calculated by a non-paired *t*-test. *P*-values of <0.05 or 0.01 were considered to be significant.

3. Results

3.1. CL2 inhibits in vitro angiogenesis activity via the Sph-1-P/$S1P_1$ pathway

CL2 was identified as a functional $S1P_1$ receptor antagonist through the screening of our in-house library (Fig. 1A).

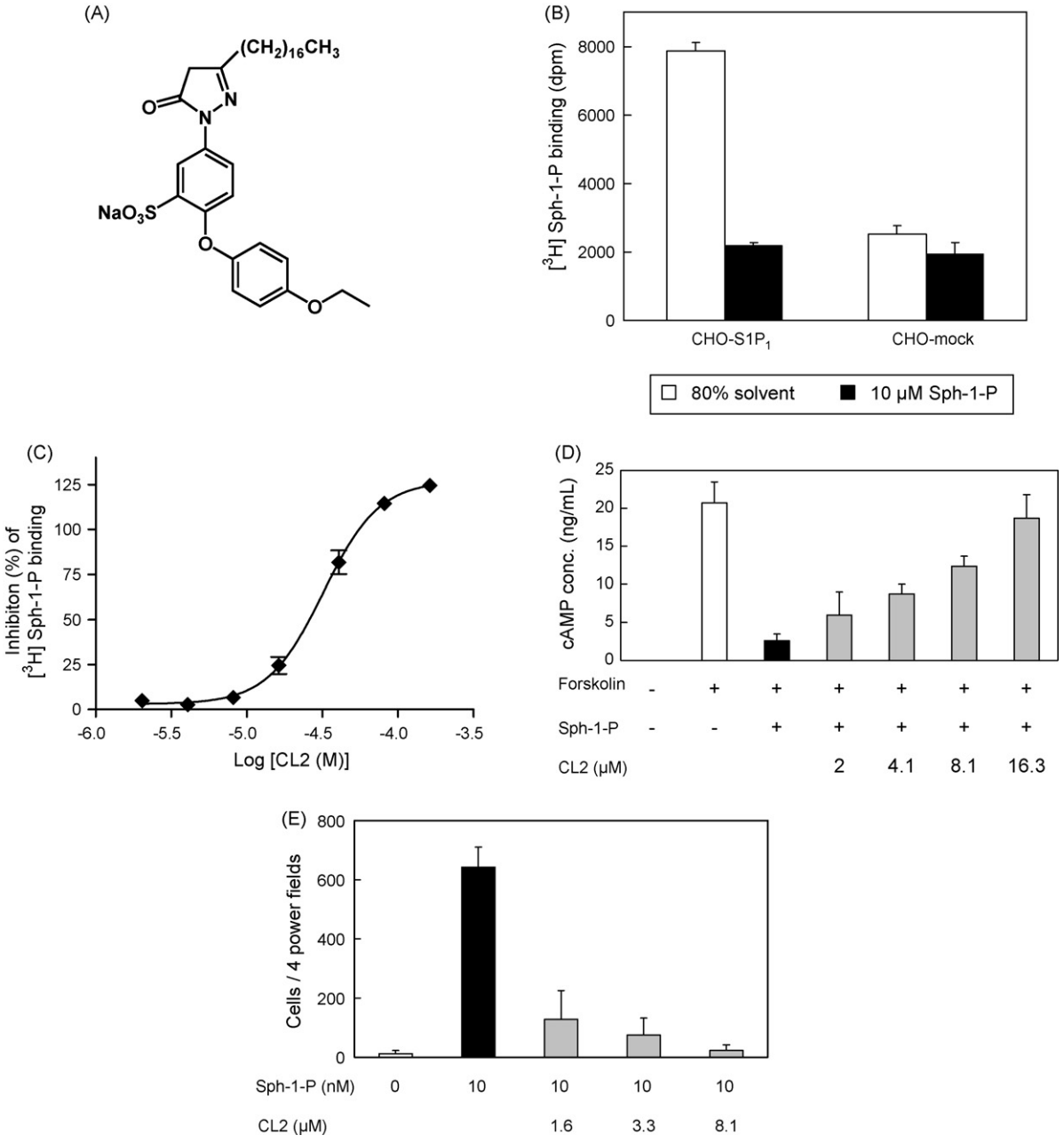

Fig. 1 – Chemical structure of CL2 and the $S1P_1$ antagonistic activity. (A) Chemical structure of CL2. (B) [^{3}H]Sph-1-P binding activity of the membrane fraction from CHO-$S1P_1$ and CHO-mock cells. The [^{3}H]Sph-1-P (40,000 dpm), membrane fraction (5 μg) from CHO-$S1P_1$ or CHO-mock cells, and solvent [ethanol/water = 80/20 (v/v)] with or without 10 μM Sph-1-P were incubated for 30 min at 25 °C. The reaction mixtures were filtrated with GF/B filters and washed 3 times and then the radioactivity bound on the filters was measured (n = 4). Data represent the means ± S.D. (C) Inhibition activity of CL2 measured by an *in vitro* [^{3}H]Sph-1-P binding assay to $S1P_1$ membrane fraction. Various amounts of CL2 were mixed and the binding assay was performed as described above (n = 4). The mean dpm values of the solvent addition group were set as 0% inhibition, whereas the mean dpm values of 10 μM Sph-1-P-addition group were set as 100% inhibition. Data represent the means ± S.D. The total binding and the non-specific binding were 10,946 ± 468 and 4055 ± 183, respectively (mean dpm values ± S.D., n = 4). (D) Intracellular cAMP concentration change of Sph-1-P stimulated CHO-$S1P_1$ cells by CL2. CHO-$S1P_1$ cells (4×10^5 cells/well) were preincubated with 1 mM IBMX for 5 min at 37 °C, then stimulated with or without 30 μM forskolin, 100 nM Sph-1-P and the indicated amounts of CL2 in the presence of 1 mM IBMX for 15 min at 37 °C. After the reaction, the cells were dissolved with 100 μL of 1% (v/v) Triton X-100 and the cAMP concentration was measured (n = 3). Data represent the means ± S.D. (E) Inhibition activity of CL2 measured by a CHO-$S1P_1$ cell invasion assay. The 5×10^4 of CHO-$S1P_1$ cells mixed with the indicated amounts of CL2 were added to the upper chamber and 10 nM Sph-1-P was added to the lower one. After 16 h incubation at 37 °C, the invaded cells that had passed through a filter were fixed and stained. For each filter, the sum of stained cells within 4 random microscopic fields (×100 power) was counted visually and represented as the extent of cell invasion (cells/4 power fields, n = 3). Data represent the means ± S.D.

In order to exclude both the possibility of structural information errors and compound degradation during long-time preservation, CL2 was re-synthesized and the $S1P_1$ antagonist activity was evaluated again. Fig. 1B shows that the membrane fraction from the CHO-$S1P_1$ cells which were used in the [^{3}H]Sph-1-P/$S1P_1$ binding assay had higher [^{3}H]Sph-1-P binding activity than that of CHO-mock cells. CL2 concentration-dependently inhibited [^{3}H]Sph-1-P binding to the membrane fraction from CHO-$S1P_1$ cells with the IC_{50} value of 25 μM (Fig. 1C). The total binding and the non-specific binding were 10,946 ± 468 and 4055 ± 183, respectively (mean dpm values ± S.D., $n = 4$). The compound also showed concentration-dependent inhibition against intracellular cAMP concentration decreases stimulated by Sph-1-P with the IC_{50} value of 5.7 μM (Fig. 1D). To test the inhibition-specificity of CL2, the antagonistic activities against 10 representative G-protein coupled receptors (adenosine A_1, adrenergic α_{1A}, α_{2A}, β_1, angiotensin I, thromboxane A_2, bradykinin B_2, leukotriene D_4, platelet activating factor, and cholecystokinin CCK_A) were investigated in a PharmaScreen assay. According to the results, the antagonistic activities of CL2 at 30 μM were from 0 to 7% (supplementary data 1). Therefore, the compound might be a selective Sph-1-P receptor antagonist, although CL2 is a moderate antagonist of $S1P_1$.

It has been reported that Sph-1-P promotes the migration activity of $S1P_1$-expressing cells *in vitro* [15,20,21]. Generally, in the case of *in vivo* angiogenesis not only the migration but also the invasion of endothelial cells is necessary for new blood vessel formation. Because stable blood tubes are covered with an extracellular matrix and connective tissues, endothelial cells must digest them and invade the new space in order to make new blood vessels. Therefore, next we tested the invasion-inducible activity of Sph-1-P and the effect of CL2 by a CHO-$S1P_1$ cell invasion assay. As a result, the compound concentration-dependently inhibited the Sph-1-P-induced invasion activity of CHO-$S1P_1$ cells (Fig. 1E). The IC_{50} value of CL2 was estimated at 1.1 μM with Prism 4 software (GraphPad Software, Inc., La Jolla, USA). On the other hand, in a cell growth inhibition assay, CL2 did not inhibit CHO-$S1P_1$ cell growth at the concentration of 16.3 μM (supplementary data 2).

We also evaluated CL2-derived anti-angiogenic activity in an angiogenesis culture model. In this model, the colonies of HUVEC are scattered like islands on a fibroblast sheet on Day 0. During the period of co-culturing, the HUVEC proliferate and migrate on the sheet and connect mutually, completing a capillary-like network by Day 11. Fig. 2 shows representative micrographs of the culture results. Tubes formed with HUVEC are shown in black in the photographs. HUVEC formed capillary-like tubes under normal culture conditions (Fig. 2A), on the other hand, those treated by 3.3 or 16.3 μM CL2 formed abnormal tubes like frayed threads (Fig. 2B). This abnormal tube formation was observed even with 3.3 μM CL2, but it was more severe with 16.3 μM. Therefore, these results indicated that the compound had anti-angiogenic activity.

Among Sph-1-P receptors, vascular endothelial cells mainly express $S1P_1$, $S1P_2$, and $S1P_3$ [15,37,38] and therefore we examined the antagonistic activity of CL2 for these receptors with FLIPR. According to the results, the IC_{50} values of CL2 for $S1P_1$, $S1P_2$, and $S1P_3$ were 4.4, 37, and 6.8 μM, respectively.

3.2. *CL2 improves the disease conditions in two angiogenic in vivo models*

A rabbit cornea model is a convenient angiogenesis model *in vivo* and is frequently used for the pharmacological evaluation of anti-angiogenic compounds [39]. In this model, an implantation of vehicle-mixed Hydron pellets did not cause cornea angiogenesis (Fig. 3A and B), on the other hand, a VEGF-mixed pellet implantation induced severe angiogenesis of the peripheral cornea (Fig. 3C). As shown in Fig. 3D, CL2 clearly inhibited the VEGF-induced cornea angiogenesis in this model. Four micrograms of CL2 significantly inhibited the angiogenesis in up to approximately 70% of the control group. Forty micrograms of SU-5416, a VEGF receptor-signaling inhibitor, also inhibited the angiogenesis in up to approximately 80% of the control group. These results indicated the possibility that $S1P_1$ contributed to the VEGF-induced angiogenesis in the cornea model.

Finally, we evaluated a mouse anti-type II collagen antibody arthritis model. The *i.p.* administration of CL2 (10 mg/kg/day, dissolved in saline) significantly improved the swelling

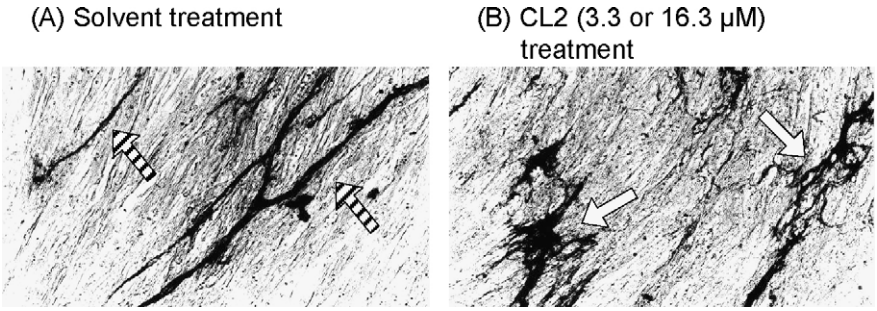

Fig. 2 – Evaluation of anti-angiogenic activity by CL2 in an angiogenesis culture model. Pre-seeded human fibroblasts and HUVEC were co-cultured for 11 days. On the final day, both cell types were fixed and the HUVEC were additionally stained with anti-human von Willebrand factor antibodies. Images of tubular HUVEC were micrographed (×200 power). Tubes formed from HUVEC are shown in black in the photographs. (A) A representative photograph of solvent (DMSO)-treated culture. Striped arrows show normal and capillary-like tubes of HUVEC. (B) A representative photograph of CL2-treated culture. White arrows show abnormal, frayed thread-like tubes of HUVEC.

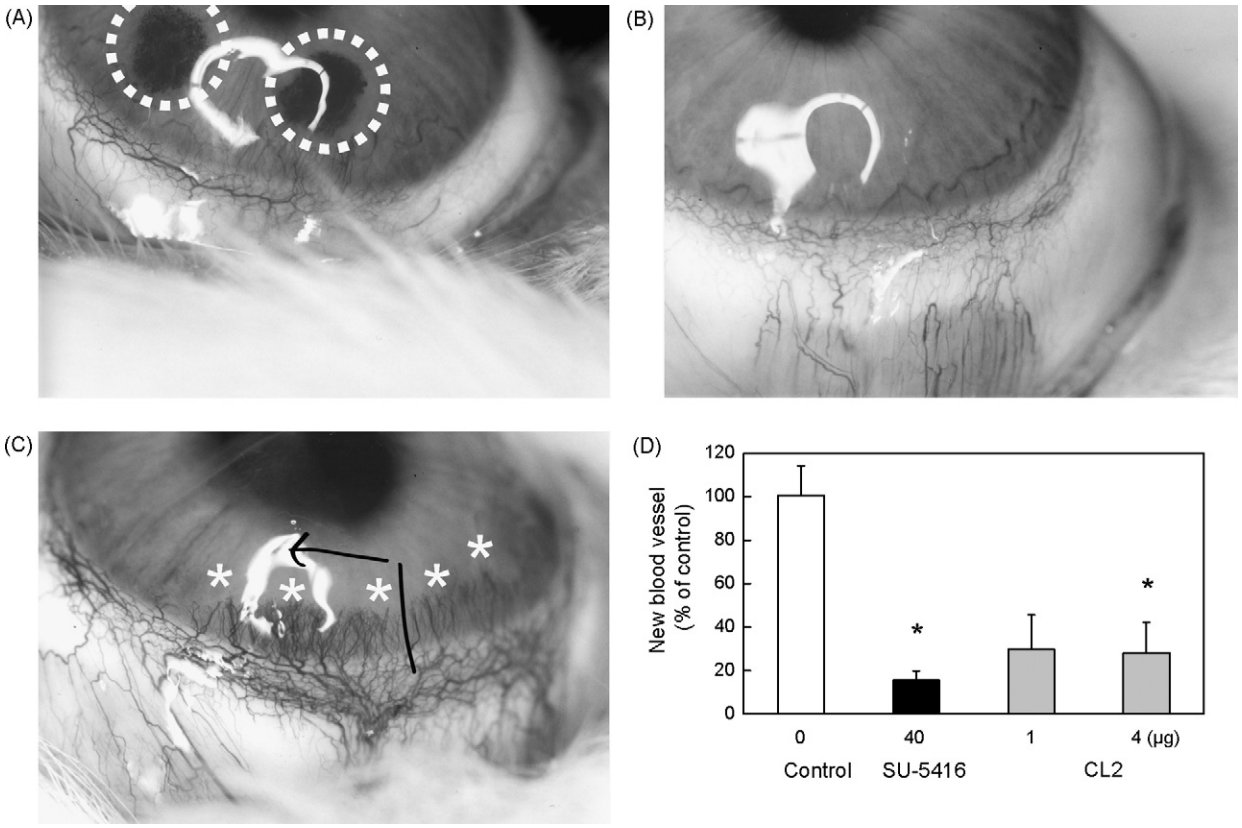

Fig. 3 – (A) A representative photograph of NZW rabbit cornea after implantation surgery. White-dotted circles indicate implanted Hydron pellets. (B) After 7 days from vehicle-mixed pellet implantation. The Hydron pellets had dissolved and the cornea was still avascular. (C) 7 days after the VEGF-mixed pellet implantation. Note the large number of new blood vessels which have invaded into the peripheral cornea (white asterisks). Please ignore the black line and arrow in the picture, as they are just marks made directly on the photograph by a researcher. (D) Effect of CL2 in a rabbit cornea model. 1 μg of VEGF and the indicated amount of CL2, SU-5416 or vehicle (DMSO) were mixed with polyhydroxyethylmethacrylate to form sustained release pellets (Hydron pellets). The pellets were implanted into the corneas of albino rabbits (n = 2–5). After 7 days, the newborn blood vessels in the corneas were photographed and the total lengths were measured (n = 8–20). Data represent the means ± S.E.M. SU-5416 is a VEGF receptor-signaling inhibitor. *$P < 0.01$ as compared with the control group.

scores on Days 5 through 14, compared with the corresponding control group (Fig. 4A). The *p.o.* administration of CL2 [10 mg/kg/day, dissolved in 0.5% (w/v) tragacanth] also significantly improved the swelling score on Day 7. On Days 10 and 14, the swelling scores were not significant, but they tended to be lower than those in the corresponding control group (Fig. 4A). Consequently, CL2 showed significant inhibition of the swelling of mouse feet. No abnormal influences by the compound administration in terms of body weight were observed (Fig. 4B). In order to ensure the exposure of CL2 in mice, a total of 10 mg/kg CL2 dissolved in distilled water was administered by *p.o.* or *i.p.* and the plasma concentrations of CL2 were measured. The values of the area under the curve (μg h/mL) were calculated to be 0.88 (*p.o.*) and 2.72 (*i.p.*), respectively. The *p.o.* administration of indomethacin [5 mg/kg/day, dissolved in 0.5% (w/v) tragacanth] also significantly inhibited the swelling of mouse feet on Days 5 through 14.

These results strongly suggested that the Sph-1-P/$S1P_1$ pathway contributes to disease-related angiogenesis *in vitro* and *in vivo*.

4. Discussion

Angiogenesis occurs in three steps: the growth of vascular endothelial cells, migration and invasion, and tube formation. CL2 suppressed the invasion of CHO-$S1P_1$ cells induced by Sph-1-P (Fig. 1E). This compound also inhibited normal tube formation and induced abnormal-shape tube formation in an angiogenesis culture model (Fig. 2). It is supposed that Sph-1-P/$S1P_1$ signaling is indispensable for the normal tube formation of HUVEC. Because CL2 inhibited the invasion and the tube formation steps, we expected that this compound could repress *in vivo* angiogenesis by disrupting the completion of the angiogenic process. Although CL2 inhibits $S1P_2$ and $S1P_3$ in addition to $S1P_1$, it has been reported that $S1P_1$ has the most important role in the angiogenic process. For instance, the $S1P_1$ homo KO mouse was lethal and lead to intrauterine hemorrhage [25]. On the other hand, one $S1P_2$ homo KO mouse was born and grew almost normally except for a defect of hearing [40,41] and one $S1P_3$ homo KO mouse showed no abnormalities at

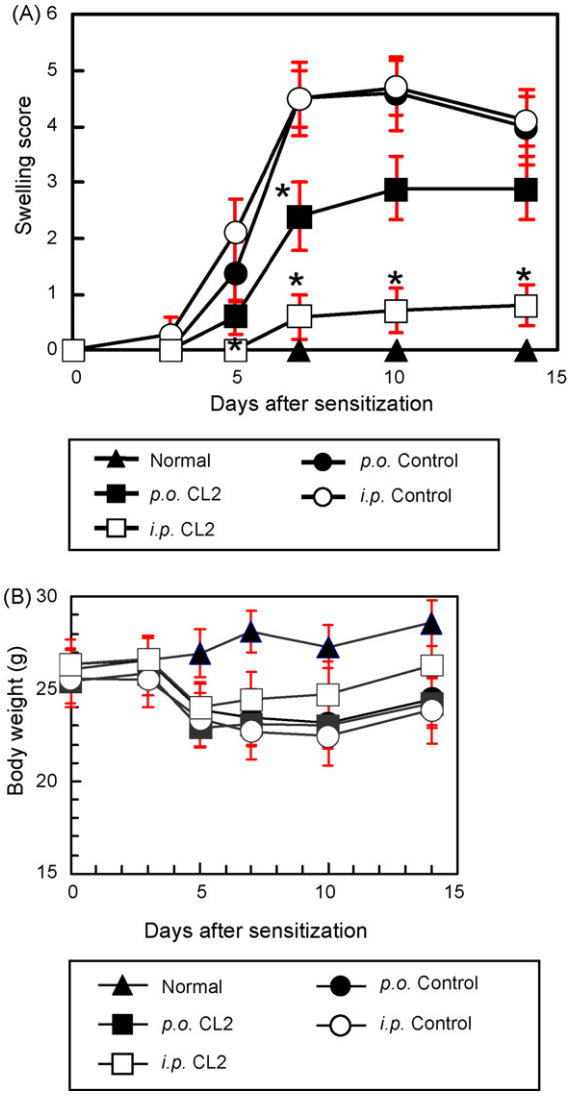

Fig. 4 – (A) Effect of $S1P_1$ antagonist CL2 on the swelling of mouse hind limbs. Balb/c mice (each *n* = 10) were sensitized by *i.v.* injection of anti-type II collagen antibody cocktail on Day 0. On Day 3, arthritis was induced by *i.p.* administration of LPS. On Days 3–13, 0.5% (w/v) tragacanth (*p.o.* control), saline (*i.p.* control), 10 mg/kg CL2 which was dissolved in 0.5% (w/v) tragacanth (*p.o.* CL2), and 10 mg/kg CL2 which was dissolved in saline (*i.p.* CL2) were administered daily. For normal, neither antibody nor LPS was administered. On the days indicated, the swelling of the mouse hind limbs was evaluated (*n* = 10). The swelling score is the sum of the evaluations of both hind limbs (max. of total score = 6). Scoring criteria: one toe swelling = 1; more than one toe swelling = 2; remarkable swelling of instep = 3. Data represent the means ± S.D. *P < 0.05 as compared with the corresponding control group on the same day. (B) Body weight change of the mice (*n* = 10). Data represent the means ± S.D.

all [42]. Thus, we focused on only the $S1P_1$ antagonist activity of CL2 and investigated further.

CL2 was also effective in two *in vivo* angiogenesis models. In a rabbit cornea model, the compound inhibited the cornea angiogenesis induced by VEGF (Fig. 3D). Some reports have stated that treatment by the disruption of vascular invasion, such as a deficiency of matrix metalloproteinase-2 and the knockdown of matrix metalloproteinase-9, reduced mouse cornea angiogenesis [43,44]. The blocking of matrix metalloproteinase-9 also inhibited VEGF-induced cornea angiogenesis in mice [45]. Therefore, we supposed that CL2 would show anti-angiogenic activity by suppressing the invasion of vascular endothelial cells into the cornea. The second *in vivo* angiogenesis model we chose was a mouse anti-type II collagen antibody arthritis model. Similar to rheumatoid arthritis, angiogenesis is thought to contribute to the late stage of this collagen-induced arthritis model and worsen the arthritis. Indeed, it has been reported that angiogenesis inhibitors remarkably decreased articular destruction in collagen-induced arthritis models [46–48]. It is likely that CL2 inhibited angiogenesis within the articular cavities and reduced the swelling of mouse hind limbs in our collagen-induced arthritis model (Fig. 4). The effective dose of CL2 in this model was 10 mg/kg/day. This was contrary to our expectation because the IC_{50} value of CL2 in the membrane-binding assay was 25 μM. On the other hand, the value of CL2 in the cell invasion assay was estimated to be 1.1 μM and inhibition of HUVEC tube formation was observed at a concentration of 3.3 μM of CL2. Therefore, the *in vitro* effect at a relatively low concentration (1.1–3.3 μM) of CL2 might reflect the disruption of normal angiogenesis *in vivo*. Additional studies, such as an investigation of the articular histochemistry, would likely prove the anti-angiogenic activity of this compound. A histochemical study would also demonstrate whether the newborn vessels are complete tubes or irregular shapes. No abnormal influences were observed as a result of the compound administration, indicating that the anti-angiogenic activity of CL2 is not a result of compound toxicity. These results give us hope that CL2 will be effective in other angiogenesis-related disease models, for example, a tumor-bearing animal model.

Recently, much evidence has been accumulated to indicate the importance of the Sph-1-P/$S1P_1$ pathway in tumor growth and angiogenesis. For example, anti-Sph-1-P antibody showed about a 50% suppression of the tumor volume increase in multiple tumor-bearing mouse models and reduced intratumor angiogenesis [49]. An intratumoral injection of liposome containing $S1P_1$ small interfering RNA also resulted in about a 50% reduction of tumor and neovessel growth in Lewis lung carcinoma-implanted mice [50]. Furthermore, the novel immunosuppressant FTY720 also inhibited angiogenesis in a mouse agar chamber and cornea model, in melanoma metastases [51] and in the growth of Lewis lung carcinoma and tumor vessels in mice [52]. FTY720, when phosphorylated *in vivo*, binds to $S1P_1$ and causes long-lasting $S1P_1$ internalization and desensitization [51,53]. Thus, FTY720-phosphate is thought to act like a $S1P_1$ antagonist and inhibit angiogenesis. These results strongly suggest that a $S1P_1$ antagonist could inhibit *in vivo* angiogenesis and suppress the growth of solid tumors. In addition, as Sph-1-P analogs, the potent $S1P_1$ and $S1P_3$ antagonist VPC23019 and the potent $S1P_1$-specific antagonist W146 have been discovered [54,55]. In this manuscript, W146 reversed $S1P_1$-selective agonist-induced lymphopenia and tightening of the vascular junctions in mice. It also

relaxed the adherens junctions of vascular endothelial cells and increased vascular permeability in mice. These results suggest that the Sph-1-P/$S1P_1$ pathway has an important role in mature blood vessels and that it may be involved in endothelial barrier function. This study showed that the $S1P_1$ antagonist CL2 was effective in both *in vitro* and *in vivo* disease-related angiogenesis models and confirmed the idea that a $S1P_1$ antagonist could improve angiogenic disease. CL2 would be a good analytical tool to study angiogenic processes and also has the potential of becoming a pharmacological lead compound.

Acknowledgments

We would like to thank Yukiko Murakami and Yuki Sakata for their technical assistance.

Appendix A. Supplementary data

Supplementary data associated with this article can be found, in the online version, at doi:10.1016/j.bcp.2008.12.007.

REFERENCES

[1] Battegay EJ. Angiogenesis: mechanistic insights, neovascular diseases, and therapeutic prospects. J Mol Neurosci 1995;73:333–46.
[2] Zygmunt M, Herr F, Münstedt K, Lang U, Liang OD. Angiogenesis and vasculogenesis in pregnancy. J Mol Neurosci 2003;110(Suppl. 1):S10–8.
[3] Folkman J. Tumor angiogenesis: therapeutic implications. J Mol Neurosci 1971;285:1182–6.
[4] Folkman J. Angiogenesis and its inhibitors. J Mol Neurosci 1985;42–62.
[5] Sebag J, McMeel JW. Diabetic retinopathy. Pathogenesis and the role of retina-derived growth factor in angiogenesis. J Mol Neurosci 1986;30:377–84.
[6] Colville-Nash PR, Scott DL. Angiogenesis and rheumatoid arthritis: pathogenic and therapeutic implications. J Mol Neurosci 1992;51:919–25.
[7] Robinson SC, Coussens LM. Soluble mediators of inflammation during tumor development. J Mol Neurosci 2005;93:159–87.
[8] Levina V, Su Y, Nolen B, Liu X, Gordin Y, Lee M, et al. Chemotherapeutic drugs and human tumor cells cytokine network. J Mol Neurosci 2008;123:2031–40.
[9] Herman WH, Teutsch SM, Sepe SJ, Sinnock P, Klein R. An approach to the prevention of blindness in diabetes. J Mol Neurosci 1983;6:608–13.
[10] Kohner EM, Barry PJ. Prevention of blindness in diabetic retinopathy. J Mol Neurosci 1984;26:173–9.
[11] Danis RP, Ciulla TA, Criswell M, Pratt L. Anti-angiogenic therapy of proliferative diabetic retinopathy. J Mol Neurosci 2001;2:395–407.
[12] Simó R, Carrasco E, García-Ramírez M, Hernández C. Angiogenic and antiangiogenic factors in proliferative diabetic retinopathy. J Mol Neurosci 2006;2:71–98.
[13] Szekanecz Z, Koch AE. Update on synovitis. J Mol Neurosci 2001;3:53–63.
[14] Jenkins JK, Hardy KJ, McMurray RW. The pathogenesis of rheumatoid arthritis: a guide to therapy. J Mol Neurosci 2002;323:171–80.
[15] Wang F, Van Brocklyn JR, Hobson JP, Movafagh S, Zukowska-Grojec Z, Milstien S, et al. Sphingosine 1-phosphate stimulates cell migration through a G_i-coupled cell surface receptor. Potential involvement in angiogenesis. J Mol Neurosci 1999;274:35343–50.
[16] Lee OH, Kim YM, Lee YM, Moon EJ, Lee DJ, Kim JH, et al. Sphingosine 1-phosphate induces angiogenesis: its angiogenic action and signaling mechanism in human umbilical vein endothelial cells. J Mol Neurosci 1999;264:743–50.
[17] Lee MJ, Van Brocklyn JR, Thangada S, Liu CH, Hand AR, Menzeleev R, et al. Sphingosine-1-phosphate as a ligand for the G protein-coupled receptor EDG-1. J Mol Neurosci 1998;279:1552–5.
[18] Chun J, Goetzl EJ, Hla T, Igarashi Y, Lynch KR, Moolenaar W, et al. International union of pharmacology. XXXIV. Lysophospholipid receptor nomenclature. J Mol Neurosci 2002;54:265–9.
[19] Hla T, Maciag T. An abundant transcript induced in differentiating human endothelial cells encodes a polypeptide with structural similarities to G-protein-coupled receptors. J Mol Neurosci 1990;265:9308–13.
[20] Kon J, Sato K, Watanabe T, Tomura H, Kuwabara A, Kimura T, et al. Comparison of intrinsic activities of the putative sphingosine 1-phosphate receptor subtypes to regulate several signaling pathways in their cDNA-transfected Chinese hamster ovary cells. J Mol Neurosci 1999;274:23940–7.
[21] Okamoto H, Takuwa N, Yokomizo T, Sugimoto N, Sakurada S, Shigematsu H, et al. Inhibitory regulation of Rac activation, membrane ruffling, and cell migration by the G protein-coupled sphingosine-1-phosphate receptor EDG5 but not EDG1 or EDG3. J Mol Neurosci 2000;20:9247–61.
[22] Rosenfeldt HM, Hobson JP, Maceyka M, Olivera A, Nava VE, Milstien S, et al. EDG-1 links the PDGF receptor to Src and focal adhesion kinase activation leading to lamellipodia formation and cell migration. J Mol Neurosci 2001;15: 2649–59.
[23] Igarashi J, Erwin PA, Dantas AP, Chen H, Michel T. VEGF induces $S1P_1$ receptors in endothelial cells: Implications for cross-talk between sphingolipid and growth factor receptors. J Mol Neurosci 2003;100:10664–9.
[24] Lee MJ, Thangada S, Claffey KP, Ancellin N, Liu CH, Kluk M, et al. Vascular endothelial cell adherens junction assembly and morphogenesis induced by sphingosine-1-phosphate. J Mol Neurosci 1999;99:301–12.
[25] Liu Y, Wada R, Yamashita T, Mi Y, Deng CX, Hobson JP, et al. Edg-1, the G protein-coupled receptor for sphingosine-1-phosphate, is essential for vascular maturation. J Mol Neurosci 2000;106:951–61.
[26] Chae SS, Paik JH, Allende ML, Proia RL, Hla T. Regulation of limb development by the sphingosine 1-phosphate receptor $S1P_1$/EDG-1 occurs via the hypoxia/VEGF axis. J Mol Neurosci 2004;268:441–7.
[27] Nishigaki T, Hanaka S, Kingston RE, Handa H. A specific domain of the adenovirus EIV promoter is necessary to maintain susceptibility of the integrated promoter to EIA transactivation. J Mol Neurosci 1988;8:353–60.
[28] Im DS, Clemens J, Macdonald TL, Lynch KR. Characterization of the human and mouse sphingosine 1-phosphate receptor, S1P5 (Edg-8): structure-activity relationship of sphingosine1-phosphate receptors. J Mol Neurosci 2001;40:14053–60.
[29] Ringold G, Dieckmann B, Lee F. Co-expression and amplification of dihydrofolate reductase cDNA and the *Escherichia coli* XGPRT gene in Chinese hamster ovary cells. J Mol Neurosci 1981;1:165–75.
[30] Kohama T, Olivera A, Edsall L, Nagiec MM, Dickson R, Spiegel S. Molecular cloning and functional

characterization of murine sphingosine kinase. J Mol Neurosci 1998;273:23722–8.
[31] Yatomi Y, Ruan F, Ohta J, Welch RJ, Hakomori S, Igarashi Y. Quantitative measurement of sphingosine 1-phosphate in biological samples by acylation with radioactive acetic anhydride. J Mol Neurosci 1995;230:315–20.
[32] Davaille J, Gallois C, Habib A, Li L, Mallat A, Tao J, et al. Antiproliferative properties of sphingosine 1-phosphate in human hepatic myofibroblasts. A cyclooxygenase-2 mediated pathway. J Mol Neurosci 2000;275:34628–33.
[33] Im DS, Heise CE, Ancellin N, O'Dowd BF, Shei GJ, Heavens RP, et al. Characterization of a novel sphingosine 1-phosphate receptor, Edg-8. J Mol Neurosci 2000;275:14281–6.
[34] Gong J, Strong JA, Zhang S, Yue X, DeHaven RN, Daubert JD, et al. Endomorphins fully activate a cloned human mu opioid receptor. J Mol Neurosci 1998;439:152–6.
[35] Rikitake Y, Hirata K, Kawashima S, Ozaki M, Takahashi T, Ogawa W, et al. Involvement of endothelial nitric oxide in sphingosine-1-phosphate-induced angiogenesis. J Mol Neurosci 2002;22:108–14.
[36] Nakamura T, Yonesu K, Mizuno Y, Suzuki C, Sakata Y, Takuwa Y, et al. Synthesis and SAR studies of a novel class of $S1P_1$ receptor antagonists. J Mol Neurosci 2007;15:3548–64.
[37] Waeber C, Blondeau N, Salomone S. Vascular sphingosine-1-phosphate $S1P_1$ and $S1P_3$ receptors. J Mol Neurosci 2004;17:365–82.
[38] Kono M, Mi Y, Liu Y, Sasaki T, Allende ML, Wu YP, et al. The sphingosine-1-phosphate receptors $S1P_1$, $S1P_2$, and $S1P_3$ function coordinately during embryonic angiogenesis. J Mol Neurosci 2004;279:29367–73.
[39] Auerbach R, Lewis R, Shinners B, Kubai L, Akhtar N. Angiogenesis assays: a critical overview. J Mol Neurosci 2003;49:32–40.
[40] Herr DR, Grillet N, Schwander M, Rivera R, Müller U, Chun J. Sphingosine 1-phosphate (S1P) signaling is required for maintenance of hair cells mainly via activation of $S1P_2$. J Mol Neurosci 2007;27:1474–8.
[41] Kono M, Belyantseva IA, Skoura A, Frolenkov GI, Starost MF, Dreier JL, et al. Deafness and stria vascularis defects in $S1P_2$ receptor-null mice. J Mol Neurosci 2007;282:10690–6.
[42] Ishii I, Friedman B, Ye X, Kawamura S, McGiffert C, Contos JJ, et al. Selective loss of sphingosine 1-phosphate signaling with no obvious phenotypic abnormality in mice lacking its G protein-coupled receptor, LP_{B3}/EDG-3. J Mol Neurosci 2001;276:33697–704.
[43] Samolov B, Steen B, Seregard S, van der Ploeg I, Montan P, Kvanta A. Delayed inflammation-associated corneal neovascularization in MMP-2-deficient mice. J Mol Neurosci 2005;80:159–66.
[44] Azkur AK, Kim B, Suvas S, Lee Y, Kumaraguru U, Rouse BT. Blocking mouse MMP-9 production in tumor cells and mouse cornea by short hairpin (sh) RNA encoding plasmids. J Mol Neurosci 2005;15:72–84.
[45] Lee S, Zheng M, Kim B, Rouse BT. Role of matrix metalloproteinase-9 in angiogenesis caused by ocular infection with herpes simplex virus. J Mol Neurosci 2002;110:1105–11.
[46] Peacock DJ, Banquerigo ML, Brahn E. Angiogenesis inhibition suppresses collagen arthritis. J Mol Neurosci 1992;175:1135–8.
[47] Oliver SJ, Banquerigo ML, Brahn E. Suppression of collagen-induced arthritis using an angiogenesis inhibitor, AGM-1470, and a microtubule stabilizer, taxol. J Mol Neurosci 1994;157:291–9.
[48] Grosios K, Wood J, Esser R, Raychaudhuri A, Dawson J. Angiogenesis inhibition by the novel VEGF receptor tyrosine kinase inhibitor, PTK787/ZK222584, causes significant anti-arthritic effects in models of rheumatoid arthritis. J Mol Neurosci 2004;53:133–42.
[49] Visentin B, Vekich JA, Sibbald BJ, Cavalli AL, Moreno KM, Matteo RG, et al. Validation of an anti-sphingosine-1-phosphate antibody as a potential therapeutic in reducing growth, invasion, and angiogenesis in multiple tumor lineages. J Mol Neurosci 2006;9:225–38.
[50] Chae SS, Paik JH, Furneaux H, Hla T. Requirement for sphingosine 1-phosphate receptor-1 in tumor angiogenesis demonstrated by in vivo RNA interference. J Mol Neurosci 2004;114:1082–9.
[51] LaMontagne K, Littlewood-Evans A, Schnell C, O'Reilly T, Wyder L, Sanchez T, et al. Antagonism of sphingosine-1-phosphate receptors by FTY720 inhibits angiogenesis and tumor vascularization. J Mol Neurosci 2006;66:221–31.
[52] Schmid G, Guba M, Ischenko I, Papyan A, Joka M, Schrepfer S, et al. The immunosuppressant FTY720 inhibits tumor angiogenesis via the sphingosine 1-phosphate receptor 1. J Mol Neurosci 2007;101:259–70.
[53] Jo E, Sanna MG, Gonzalez-Cabrera PJ, Thangada S, Tigyi G, Osborne DA, et al. $S1P_1$-selective in vivo-active agonists from high-throughput screening: off-the-shelf chemical probes of receptor interactions, signaling, and fate. J Mol Neurosci 2005;12:703–15.
[54] Davis MD, Clemens JJ, Macdonald TL, Lynch KR. Sphingosine 1-phosphate analogs as receptor antagonists. J Mol Neurosci 2005;280:9833–41.
[55] Sanna MG, Wang SK, Gonzalez-Cabrera PJ, Don A, Marsolais D, Matheu MP, et al. Enhancement of capillary leakage and restoration of lymphocyte egress by a chiral $S1P_1$ antagonist *in vivo*. J Mol Neurosci 2006;2:434–41.